NONLINEAR DAMPED OSCILLATORS ON RIEMANNIAN MANIFOLDS: NUMERICAL SIMULATION

SIMONE FIORI *

Abstract. Nonlinear oscillators are ubiquitous in sciences, being able to model the behavior of complex nonlinear phenomena, as well as in engineering, being able to generate repeating (i.e., periodic) or non-repeating (i.e., chaotic) reference signals. The state of the classical oscillators known from the literature evolves in the space $\mathbb{R}^n$, typically with $n = 1$ (e.g., the famous van der Pol vacuum-tube model), $n = 2$ (e.g., the FitzHugh-Nagumo model of spiking neurons) or $n = 3$ (e.g., the Lorenz simplified model of turbulence). The aim of the current paper is to present a general scheme for the numerical differential-geometry-based integration of a general second-order, nonlinear oscillator model on Riemannian manifolds and to present several instances of such model on manifolds of interest in sciences and engineering, such as the Stiefel manifold and the space of symmetric, positive-definite matrices.

Key words. Chaotic system; Nonlinear autonomous oscillator; Riemannian manifold; Geometric numerical integration.

1. Introduction. Nonlinear oscillators (both autonomous and driven) have been widely studied in the scientific literature either because they arise naturally in the process of modeling complex physical structures and because they constitute the basis for several modern applications. Paradigmatic examples of nonlinear oscillators obtained from models of complex physical systems are the van der Pol oscillator, that arose from a model of vacuum tubes [29], and the Lorenz oscillator [22], that was derived from the simplified model of convection rolls in the atmosphere and has important implications in climate and weather predictions. The literature is rich in Lorenz-like systems, such as the Chen system and the Lü system [21]. Paradigmatic applications of designed oscillators (either self-sustained or controlled) is to the secure transmission of information [40], to the active damping of mechanical vibrations [9], and to the analysis of bivariate data by a coupled-oscillators approach [34]. A detailed list of applications of non-linear, chaotic, oscillators in science and engineering may be found, e.g., in the review paper [6]. We would like to cite two, in particular, that appear as especially relevant, as they relate chaos analysis with a powerful signal-processing technique known as Independent Component Analysis (ICA), namely, wearable mental-health monitoring [33], and seismic signal detection and characterization [1].

The state of nonlinear oscillators evolves over time in complex, non-repeating, deterministic patterns. Most nonlinear oscillators appear as first-order or second-order dynamical systems involving a single real variable. The simplest model is perhaps the *linear harmonic oscillator*. As no damping is present, the harmonic oscillator preserves its initial energy indefinitely. An example of 'damped' oscillator is the van der Pol oscillator model, which is closely-related to biologically-inspired nonlinear dynamical systems such as the FitzHugh-Nagumo model [16], the Hodgkin-Huxley model of the activation and deactivation dynamics of spiking neurons and the Hindmarsh-Rose model [37], that augments with a slow variable the planar FitzHugh-Nagumo model. Another well-studied nonlinear system that exhibits a complex behavior is the *Duffing oscillator* that models, for example, a spring pendulum whose spring's stiffness does not exactly obey Hooke's law [36].

Examples of dynamical systems involving more than one variable are known in the scientific literature. A nonlinear, three-dimensional, deterministic dynamical system is the *Rabinovich-Fabrikant oscillator* [30]. It is described by a set of three coupled ordinary differential equations comprising two parameters, which may exhibit a complex behavior for certain values of the parameters, while for other values of the parameters its flow may tend to a stable periodic orbit. Likewise, the *Rössler oscillator* [35] helps describing equilibrium in chemical reactions. In addition, a three-dimensional nonlinear oscillator is the

*The author is with Dipartimento di Ingegneria dell'Informazione, Facoltà di Ingegneria, Università Politecnica delle Marche, Via Brecce Bianche, Ancona I-60131, Italy. (✉ s.fiori@univpm.it). This paper should be cited as: **S. Fiori, "Nonlinear damped oscillators on Riemannian manifolds: Numerical simulation", Communications in Nonlinear Science and Numerical Simulation, Vol. 47, pp. 207 — 222, June 2017**.

Colpitts circuit, built up of a bipolar junction transistor and a resonant network consisting of an inductor and two capacitors [24].

The state of the above nonlinear oscillators recalled from the scientific literature evolves in the real line $\mathbb{R}$ or in the real plane $\mathbb{R}^2$ or in the ordinary space $\mathbb{R}^3$. As an example, the Figure 1.1 illustrates the state of an Hindmarsh-Rose model in terms of the three variables $(V, n, h) \in \mathbb{R}^3$. The present paper

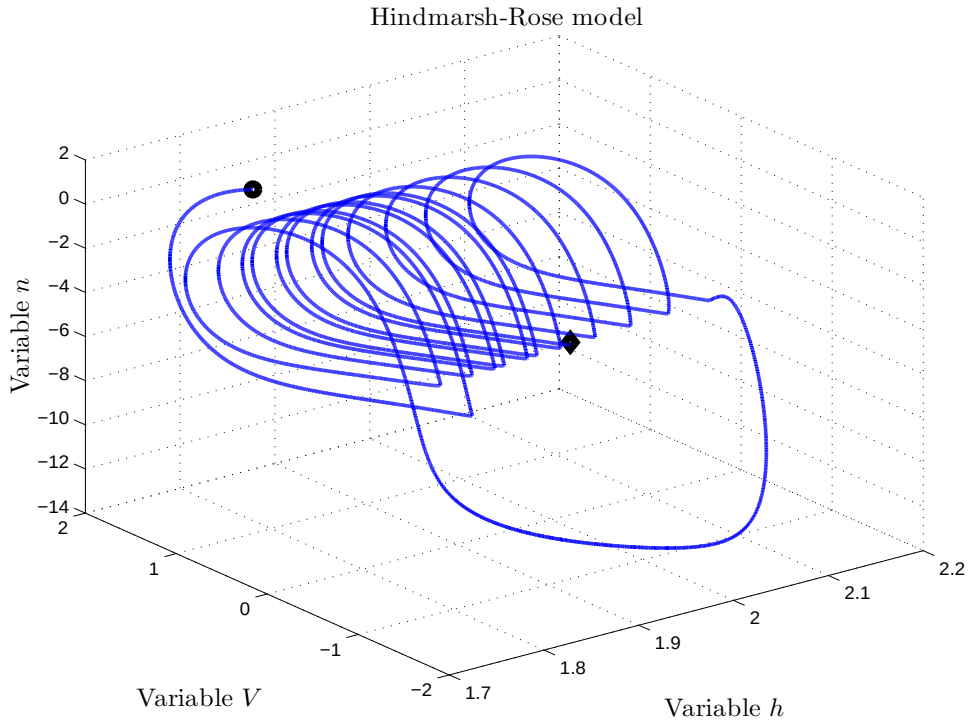

FIG. 1.1. *Exemplary behavior of an Hindmarsh-Rose model in terms of the three variables* $(V, n, h) \in \mathbb{R}^3$. *The thick circle denotes the initial point, while the thick diamond denotes the final point of the trajectory.*

aims at extending previous studies on nonlinear autonomous oscillators from flat Euclidean spaces to high-dimensional curved Riemannian manifolds. Riemannian manifolds of interest in the literature are the Stiefel manifold (along with the special cases of the unit-hypersphere and the orthogonal group), the space of symmetric, positive-definite matrices and the special orthogonal group. In particular, the current contribution aims at presenting *discrete-time* nonlinear autonomous oscillators equations that may be implemented on a computing platform and at investigating to what extent the obtained discrete-time dynamical system replicates its theoretical continuous-time differential-geometric properties.

The theory and practice of non-linear oscillators is one of the topics of prime interest in the nonlinear science community, as testified by a number of papers about non-linear oscillators in mobile robotics [5], thermodynamics [27], signal transmission and processing [39, 43], mathematical optimization [46] and artificial intelligence [44]. The motivation and fundamental aim of the present contribution is to open new perspectives in the theory of nonlinear damped oscillators on curved spaces and to promote research efforts in this field.

The current paper is organized as follows. The Section 2 recalls the notation used in differential geometry (in Subsection 2.1) and describes a general second-order dynamical system derived by the analysis of a point-wise particle sliding on a smooth manifold following the landscape of a potential energy function and under the effect of passive/active damping (in Subsection 2.2); the Subsection 2.3 illustrates

the notation and the general structure of the second-order oscillator via a 1-dimensional example. The Subsection 3.1 describes discrete-time second-order autonomous oscillators on the unit-hypersphere, the Subsection 3.2 describes oscillators on a Lie group, namely, the manifold of special orthogonal matrices, the Subsection 3.3 deals with the manifold of symmetric, positive-definite matrices, and the Subsection 3.4 illustrates discrete-time second-order autonomous oscillators on the compact Stiefel manifold, for which several quantities of interest are not available in closed form; the Subsection 3.5 discusses the problem of the (lack of) conservation of energy in theoretically-conservative systems due to finite-length stepping in discrete-time systems. The Section 4 illustrates the developed theory by means of two examples of oscillators on the sphere S^2 that allows graphical rendering. The Section 5 concludes the paper and outlines some foreseen applications and theoretical research.

2. Nonlinear autonomous oscillators on Riemannian manifolds. The present section summarizes the notation of differential geometry used throughout this paper, and describes the general structure of nonlinear, second-order, dynamical systems on Riemannian manifolds arising from the modeling of a point-wise particle sliding on a smooth manifold.

2.1. Notation of differential geometry. For the theory of differentiable manifolds, readers may consult the series of books [38].

Let M denote a real differentiable manifold of dimension r. In local coordinates, a point $x \in M$ is denoted by $(x^1, x^2, \ldots, x^r)$. At a point $x \in M$, the tangent space to the manifold M is denoted as T_xM and represents the vector space of dimension r spanned by all tangent vectors to all smooth curves on M passing through the point x. The canonical basis of a tangent space T_xM is denoted by $(\partial_1, \partial_2, \ldots, \partial_r)$ where $\partial_\sigma = \partial_\sigma(x)$. The symbol TM denotes the tangent bundle defined as $TM \stackrel{\text{def}}{=} \{(x, v) | x \in M, v \in T_xM\}$. The cotangent space to the manifold M at a point $x \in M$ is denoted as $T_x^\star M$ and represents the set of linear functions from T_xM to $\mathbb{R}$. Elements of a cotangent space are termed cotangent vectors. The canonical basis of the cotangent space $T_x^\star M$ is denoted by $(\mathrm{d}x^1, \mathrm{d}x^2, \ldots, \mathrm{d}x^r)$. In the present paper, the Einstein summation convention is in force: in an expression where repeated indexes occur, summation over those indexes is implied.

A Riemannian manifold M is endowed with a bilinear, symmetric, positive-definite form $\mathbb{G}_x : T_xM \times T_xM \to \mathbb{R}$. In local coordinates, the bilinear form $\mathbb{G}$ is expressed by the components of the metric tensor $\mathbb{G}_{\sigma\tau}(x) \stackrel{\text{def}}{=} \mathbb{G}_x(\partial_\sigma, \partial_\tau)$. Therefore, expressing two tangent vectors as $w = w^\sigma \partial_\sigma$ and $v = v^\sigma \partial_\sigma$, bilinearity implies $\mathbb{G}_x(w, v) = \mathbb{G}_{\sigma\tau}(x) w^\sigma v^\tau$. The components of the inverse metric tensor are denoted by $\mathbb{G}^{\sigma\tau}$. A local metric $\mathbb{G}_x$ also defines a local norm $\|v\|_x \stackrel{\text{def}}{=} \sqrt{\mathbb{G}_x(v, v)}$, for $v \in T_xM$.

The metric 'sharp' operator is denoted by $\mathbb{G}^\sharp$. In local coordinates, the sharp operator $\mathbb{G}_x^\sharp : T_x^\star M \to T_xM$ acts as $\mathbb{G}_x^\sharp(u_\sigma \mathrm{d}x^\sigma) = \mathbb{G}^{\sigma\tau} u_\sigma \partial_\tau$. Let $\psi : M \to \mathbb{R}$ denote a differentiable function. The differential of a function $\psi : M \to \mathbb{R}$ at a point $x \in M$ is denoted by $\mathrm{d}_x\psi \in T_x^\star M$. Given a tangent vector $v \in T_xM$, the scalar $\mathrm{d}_x\psi(v)$ represents the directional derivative of the function ψ along the direction v, namely $d_x\psi(v) = \frac{\partial \psi}{\partial x^\sigma} v^\sigma = \mathbb{G}_x((\mathbb{G}_x^\sharp \circ \mathrm{d}_x)\psi, v)$. Therefore, the Riemannian gradient of the function ψ with respect to a metric $\mathbb{G}$, evaluated at the point $x \in M$, is $(\mathbb{G}_x^\sharp \circ \mathrm{d}_x)\psi$.

The Christoffel symbols of the second kind of the Levi-Civita connection associated with the metric tensor of components $\mathbb{G}_{\sigma\tau}$ are denoted by $\overset{\mathbb{G}}{\Gamma}{}^\alpha_{\sigma\tau}$, while the associated Christoffel form $\overset{\mathbb{G}}{\Gamma}_x$ is defined (in local coordinates) by $[\overset{\mathbb{G}}{\Gamma}_x(v, w)]^\alpha \stackrel{\text{def}}{=} \Gamma^\alpha_{\sigma\tau} v^\sigma w^\tau$. A Levi-Civita connection $\overset{\mathbb{G}}{\nabla}$ defines a parallel transport operator $\overset{\mathbb{G}}{\mathrm{P}}$ that allows one to move a tangent vector along a curve on a manifold.

The notion of geodesic curve generalizes the notion of straight line of Euclidean spaces. A distinguishing feature of a straight line of an Euclidean space is that it translates parallel to itself, namely, it is *self-parallel*. The notion of 'straight line' on a curved space inherits such a distinguishing feature. A geodesic on a manifold M with connection $\overset{\mathbb{G}}{\nabla}$ and associated parallel transport operator $\overset{\mathbb{G}}{\mathrm{P}}$, is a curve γ such that $\dot\gamma$ is parallel translated along γ itself. A geodesic curve $\gamma : \mathbb{I} \to M$, with $0 \in \mathbb{I}$, that satisfies the

initial conditions $\gamma(0) = x \in M$ and $\dot{\gamma}(0) = v \in T_xM$ is denoted as $\gamma_{x,v}(t)$. Given two points $x, y \in M$, suppose that there exists a geodesic $\gamma : [0,\ 1] \to M$ that joins them, namely, such that $\gamma(0) = x$ and $\gamma(1) = y$. In this case, the special parallel transport operator $\overset{\mathbb{G}}{\mathrm{P}}_\gamma : T_xM \to T_yM$ may be denoted as $\mathrm{P}^{x \to y} : T_xM \to T_yM$, with the convention that the operator $\mathrm{P}^{x \to x}$ coincides with the identity map in T_xM.

The parallel transport operator preserves the inner products, namely, given two geodesically-connectable points $x, y \in M$ and two tangent vectors $v, w \in T_xM$, it holds that $\mathbb{G}_y(\mathrm{P}^{x \to y}(v), \mathrm{P}^{x \to y}(w)) = \mathbb{G}_x(v, w)$. In particular, taking $v = w$ shows that parallel transport preserves the norm of a tangent vector, namely, it represents an isometry.

Given a geodesic line $\gamma_{x,v}(t)$, a *manifold exponential* $\exp : TM \to M$ is defined as $\exp_x(v) \overset{\text{def}}{=} \gamma_{x,v}(1)$. It maps a tangent vector $v \in T_xM$ to a point $y = \exp_x(v)$ that belongs to a neighborhood of the point $x \in M$. Its inverse 'log' is defined only locally and is termed *manifold logarithm*. Given points $x, y \in M$, it returns a tangent vector $v = \log_x(y) \in T_xM$ such that $\exp_x(v) = y$.

Given two points $x, y \in M$ connectable by a *minimizing* geodesic line $\gamma : [0,\ 1] \to M$, the *Riemannian* distance between those points is defined by:

$$d(x, y) \overset{\text{def}}{=} \int_0^1 \sqrt{\mathbb{G}_{\gamma(t)}(\dot{\gamma}(t), \dot{\gamma}(t))}\mathrm{d}t = \| \log_x(y) \|_x. \tag{2.1}$$

A fundamental result of the calculus on manifolds states that the Riemannian gradient of a squared distance function reads:

$$\mathbb{G}_x^\sharp(\mathrm{d}_x d^2(x, y)) = -2 \log_x(y). \tag{2.2}$$

2.2. Second-order dynamical systems on Riemannian manifolds. A classical dynamical system on the space $\mathbb{R}^3$ is the Newton's law of motion of a particle of mass m subjected to an external force $f : \mathbb{R}^3 \times \mathbb{R}^3 \to \mathbb{R}^3$. The trajectory $x : \mathbb{I} \to \mathbb{R}^3$, along the time-interval $\mathbb{I}$, followed by such a particle, is computed as the solution of the Newton's equation:

$$\ddot{x} = m^{-1} f(x, \dot{x}). \tag{2.3}$$

The phase-space of the dynamical system (2.3), namely, the high-dimensional space of the kinematic states of the particle, is given by $\mathbb{R}^3 \times \mathbb{R}^3$. The term $\ddot{x}(t)$ denotes the instantaneous acceleration of the particle at the time t, the mass term m accounts for the inertia of the particle and the external force f depends on the instantaneous position $x(t)$ and on the instantaneous velocity $\dot{x}(t)$.

By embedding the manifold M into an Euclidean space of sufficient size, the dynamics of a point-wise particle sliding on a Riemannian manifold M with metric $\mathbb{G}$ may be expressed, in embedded coordinates, as:

$$\begin{cases} \dot{x} = v, \\ \dot{v} + \overset{\mathbb{G}}{\Gamma}_x(v, v) = -(\mathbb{G}_x^\sharp \circ \mathrm{d}_x) V_x + \mathbb{G}_x^\sharp(f_x), \end{cases} \tag{2.4}$$

in the tangent-bundle variables $(x(t), v(t)) \in TM$. Such fundamental equations were derived in [15]. The tangent bundle plays the role of phase-space for the dynamical system (2.4). The role of 'mass' is played by the inverse inertia tensor $\mathbb{G}_x^\sharp$, while the manifold-valued variable x plays the role of instantaneous position on the manifold M, the tangent-bundle variable v plays the role of instantaneous velocity of the particle, and the term $\dot{v} + \overset{\mathbb{G}}{\Gamma}_x(v, v)$ is termed instantaneous geometric acceleration.

In the context of autonomous dynamical systems subjected to external driving forces on manifolds, a *force* at a point $x \in M$ is a cotangent vector, namely $f_x : T_xM \to T_x^\star M$. The force $f_x = f_x(v) \in T_x^\star M$ will essentially represent damping effects (either dissipative and active), specifically:

- *Friction-type damping*: This kind of damping generalizes the Rayleigh damping [25] and is expressed by the forcing term $f_x = -\frac{1}{2}\mu \frac{\partial(\mathbb{G}_x(v,v)^\epsilon)}{\partial v^\sigma} \mathrm{d}x^\sigma$, with $\epsilon \geq 1$ being a damping coefficient and $\mu \geq 0$ being a viscosity coefficient. The generalized Rayleigh damping force gives rise to the term $\mathbb{G}_x^\sharp(f_x) = -\mu \|v\|_x^{2(\epsilon-1)} v$.
- *Active damping*: It generalizes the nonlinear damping term that appears, for example, in the van der Pol system and in the Lorenz system, and gives rise to the expression $\mathbb{G}_x^\sharp(f_x) = -\varphi_x(v)$, with $\varphi : TM \to TM$.

The *kinetic energy function* for a point-wise particle associated with the metric $\mathbb{G}$ is denoted by $K : TM \to \mathbb{R}$ and is defined by $K_x(v) \stackrel{\text{def}}{=} \frac{1}{2}\mathbb{G}_x(v,v)$ for $(x,v) \in TM$. The *potential energy function* (p.e.f.) $V : M \to \mathbb{R}$ depends on the coordinate $x \in M$ only. In the absence of any external solicitation, the dynamical system generates a trajectory $\gamma : \mathbb{I} \to M$ that follows the landscape of the potential energy function.

An example of p.e.f. is the *potential energy function of the Simple Pendulum*, defined as

$$V_x^{(\mathrm{SP})} \stackrel{\text{def}}{=} \kappa(1 - \cos d(x,r)), \tag{2.5}$$

with $\kappa > 0$ being a constant parameter and $r \in M$ denoting a reference point, whose Riemannian gradient reads

$$\mathbb{G}_x^\sharp(\mathrm{d}_x V_x^{(\mathrm{SP})}) = -\kappa \, \log_x(r) \operatorname{sinc} d(x,r), \tag{2.6}$$

where the symbol 'sinc' denotes the cardinal sine function defined as

$$\operatorname{sinc}(z) = \begin{cases} z^{-1}\sin z & \text{for } z \neq 0, \\ 1 & \text{for } z = 0. \end{cases}$$

Further examples of p.e.f.'s are the *Quadratic potential energy function*

$$V_x^{(\mathrm{II})} \stackrel{\text{def}}{=} \tfrac{1}{2}\kappa d^2(x,r), \tag{2.7}$$

with $\kappa > 0$ being a constant parameter and $r \in M$ denoting a reference point, and the *Quartic potential energy function*:

$$V_x^{(\mathrm{IV})} = \pm\tfrac{1}{2} d^2(x,r) \pm \tfrac{1}{4}\kappa d^4(x,r), \tag{2.8}$$

where $\kappa > 0$ and $r \in M$ denotes a reference point, where the signs $\pm$ were introduced to account for the *soft* and the *double-well* Duffing oscillator, together with the *hard* Duffing oscillator analyzed in [26]; the Riemannian gradient of the p.e.f. $V_x^{(\mathrm{IV})}$ reads

$$\mathbb{G}_x^\sharp(\mathrm{d}_x V_x^{(\mathrm{IV})}) = \mp[1 \pm \kappa d^2(x,r)] \log_x(r). \tag{2.9}$$

The total energy (or Hamiltonian function) $H : TM \to \mathbb{R}$ of the particle sliding on the manifold is defined by:

$$H_x \stackrel{\text{def}}{=} K_x + V_x. \tag{2.10}$$

Over a trajectory $x : \mathbb{I} \to M$ of the system (2.4), the total energy of the system varies according to the following power law:

$$\frac{\mathrm{d}H_x}{\mathrm{d}t} = \mathbb{G}_x(\mathbb{G}_x^\sharp(f_x), v). \tag{2.11}$$

If the external forcing is absent, the system (2.4) is conservative as the total energy H_x keeps constant over time; otherwise, the system is non-conservative and its energy varies over time according to the structure of the forcing term f_x. Rayleigh damping gives rise to the power term $-\mu\|v\|_x^{2\epsilon}$, that is certainly negative or zero, hence it represents an energy loss. The active damping may take energy out from the system as well as bring energy into the system, depending on the structure of the function φ. Active damping is, indeed, responsible of self-sustained oscillations.

2.3. Example: Second-order dynamical systems on 1-dimensional Riemannian manifolds. To exemplify the above theoretical development, the present subsection discusses the special case of Riemannian manifolds M of dimension 1. The main interest on such kind of manifolds is analytic tractability and the possibility to connect the study of their behavior with known results from the scientific literature on the theory of classical nonlinear damped oscillators. Examples of 1-dimensional manifolds are the unit sphere S^1 and the special orthogonal group $\mathrm{SO}(2)$.

In order to particularize the general equations (2.4) to the case of a 1-dimensional Riemannian manifold, the following preliminary observations are in order. On a Riemannian manifold M of dimension 1, the tangent space T_xM is a linear space of dimension 1 whose basis vector is denoted by ∂_x, and the metric tensor $\mathbb{G}_x$ collapses into a scalar function $g_x > 0$, $x \in M$. Given two tangent vectors $v\partial_x, w\partial_x \in T_xM$, their inner product $\mathbb{G}_x(v\partial_x, w\partial_x) = g_x vw$. Consequently, the squared norm $\|v\partial_x\|_x^2$ equals $g_x v^2$. Likewise, the cotangent space $T_x^\star M$ has dimension 1 and its basis vector is denoted by $\mathrm{d}x$. Given a cotangent vector $u\mathrm{d}x$, it holds that $\mathbb{G}_x^\sharp(u\mathrm{d}x) = \frac{u}{g_x}\partial_x$. The Christoffel symbols of the second kind of the Levi-Civita connection associated with the metric tensor $\mathbb{G}$ are computed, in general, by the formula:

$$\overset{\mathbb{G}}{\Gamma}{}_{\sigma\tau}^{\alpha} \overset{\text{def}}{=} \tfrac{1}{2}\mathbb{G}^{\alpha\beta}\left(\frac{\partial \mathbb{G}_{\beta\tau}}{\partial x^\sigma} + \frac{\partial \mathbb{G}_{\sigma\beta}}{\partial x^\tau} - \frac{\partial \mathbb{G}_{\sigma\tau}}{\partial x^\beta}\right). \tag{2.12}$$

Hence, in the present example, the only Christoffel symbol $\overset{\mathbb{G}}{\Gamma}{}_{11}^{1}$ reads $\overset{\mathbb{G}}{\gamma}_x \overset{\text{def}}{=} \frac{1}{2}\frac{1}{g_x}\frac{\mathrm{d}g_x}{\mathrm{d}x} = \frac{1}{2}\frac{\mathrm{d}\log g_x}{\mathrm{d}x}$ and the only non-zero value of the Christoffel form $\overset{\mathbb{G}}{\Gamma}_x(v\partial_x, w\partial_x)$ is $\overset{\mathbb{G}}{\gamma}_x vw$. Given a potential energy function $V : M \to \mathbb{R}$, the only non-zero component of its gradient $\mathbb{G}_x^\sharp(\mathrm{d}_x V_x)$ equals $\frac{1}{g_x}\frac{\mathrm{d}V_x}{\mathrm{d}x}$. The general equations (2.4), particularized to a 1-dimensional Riemannian manifold, read:

$$\left\{\begin{array}{rcl} \dot{x} &=& v, \\ \dot{v} &=& -\overset{\mathbb{G}}{\gamma}_x v^2 - \frac{1}{g_x}\frac{\mathrm{d}V_x}{\mathrm{d}x} - \mu(g_x v^2)^{\epsilon-1}v - \varphi_x(v). \end{array}\right. \tag{2.13}$$

An interesting special case is the one where the metric is independent of the position, namely $g_x = 1$, that implies $\overset{\mathbb{G}}{\gamma}_x = 0$. In this case, the dynamical system (2.13) particularizes to:

$$\left\{\begin{array}{rcl} \dot{x} &=& v, \\ \dot{v} &=& -\frac{\mathrm{d}V_x}{\mathrm{d}x} - \mu v^{2(\epsilon-1)}v - \varphi_x(v). \end{array}\right. \tag{2.14}$$

The above dynamical system is a prototype for the classical nonlinear damped oscillators recalled in the Introduction, such as the van der Pol oscillator and the simple pendulum.

The sphere S^1 embedded in $\mathbb{R}^2$ may be described as the set of vectors of the form $[\cos x \ \sin x]^T$, with $x \in \mathbb{R}$. It holds:

$$\frac{\mathrm{d}}{\mathrm{d}t}\begin{bmatrix} \cos x \\ \sin x \end{bmatrix} = \dot{x}\begin{bmatrix} -\sin x \\ \cos x \end{bmatrix} = v\partial_x,$$

where $v = \dot{x}$ and $\partial_x = [-\sin x \ \ \cos x]^T$. Choosing the Euclidean inner product on the tangent spaces $T_x\mathrm{S}^1$, it holds that $g_x = \mathbb{G}_x(\partial_x, \partial_x) = [-\sin x \ \ \cos x][-\sin x \ \ \cos x]^T = 1$. Hence, the dynamical equations on S^1 endowed with the Euclidean product are as in (2.14).

The exponential map corresponding to the above geometric setting may be expressed as:

$$\exp_x(v\partial_x) = \cos(v)x + \sin(v)\partial_x. \tag{2.15}$$

Given two points $y, z \in \mathrm{S}^1$, solving the equation $z = \exp_y(v\partial_y)$ in the unknown v gives $v = \arccos(z^T y)$, hence:

$$\log_y(z) = \arccos(z^T y)\partial_y, \tag{2.16}$$

and the geodesic distance between the points x and z is given by:

$$d(z,y) = |\arccos(z^T y)|. \tag{2.17}$$

In the above expressions, the superscript ^{T} denotes matrix transpose and the symbol 'arccos' denotes the inverse cosine function. The tangent spaces have the structure $T_x\mathrm{S}^{n-1} = \{v \in \mathbb{R}^n | v^T x = 0\}$. Parametrizing the point y by $[\cos x \ \sin x]^T$ and the point z by $[\cos r \ \sin r]^T$, the squared geodesic distance may be written as $d^2(z,y) = (x-r)^2$.

3. Discrete-time oscillators on special manifolds. The numerical integration of the differential equations describing non-linear oscillators on the spaces $\mathbb{R}^n$ is challenging and requires some specific numerical techniques [45]. Likewise, the numerical integration of the differential system (2.4) on specific curved manifolds of interest may be tackled by geometrically-sound integration techniques. In a numerical setting, the continuous-time state-pair function $\mathbb{I} \ni t \mapsto (x(t), v(t)) \in TM$ is replaced by a discrete-time state-pair sequence $\mathbb{N} \ni k \mapsto (x_k, v_k) \in TM$.

A discrete-time rule to solve numerically a differential equation of the type $\dot{x} = v$ on a flat space prescribes to move forward the point x_k to the point x_{k+1} along a straight line of direction v_k. By replacing the notion of straight line with the notion of geodesic line, the following (inherently nonlinear) discrete-time rule is obtained:

$$x_{k+1} = \exp_{x_k}(h\, v_k), \tag{3.1}$$

where the time-interval $h > 0$ denotes a time-discretization stepsize. In a more sophisticated setting, the geodesic line could be replaced by a Riemannian polynomial (see, for example, the study [2] on the geometry of Riemannian cubic polynomials), although one such numerical solution is not made use of in the present paper. Likewise, the notion of geodesic stepping might be generalized by the notion of retraction-based stepping [13, 19].

In order to solve the differential equation on the variable v on the tangent bundle of a general manifold, the notion of parallel transport needs to be invoked. In fact, the geometric velocity's continuous-time evolution equation on the tangent bundle is either a differential equation on a collection of linear spaces or a differential equation on a single linear space, hence, it may be solved numerically by a Euler-like discrete stepping method with the 'correction' of parallel transport. In fact, consider the tangent-bundle differential equation $\dot{v} = F(x,v)$, where $x(t) \in M$, $v(t) \in T_{x(t)}M$ and $F : TM \to TM$. The first time-derivative of the field $v(t)$ may be approximated via a finite-difference method corrected for the curvature of the manifold M as follows:

$$\frac{\mathrm{d}}{\mathrm{d}t} v(t) \approx \frac{\overset{\mathbb{G}}{\mathrm{P}}{}^{t+h\to t}[v(t+h)] - v(t)}{h},$$

where $h > 0$ denotes a discretization stepsize. (This is, in fact, an approximation of the covariant derivative of the vector field v.) Note that it would not be geometrically sound to compare the tangent vectors $v(t+h)$ and $v(t)$ because, on a curved manifold, they belong to different tangent spaces. By using the discrete-time notation x_k and v_k for the state-variables, the differential equation $\dot{v} = F(x,v)$ is approximated as:

$$\frac{\overset{\mathbb{G}}{\mathrm{P}}{}^{x_{k+1}\to x_k}(v_{k+1}) - v_k}{h} = F(x_k, v_k).$$

By making explicit the value v_{k+1}, one gets the parallel-transported forward Euler stepping method:

$$v_{k+1} = \overset{\mathbb{G}}{\mathrm{P}}{}^{x_k \to x_{k+1}}[v_k + hF(x_k, v_k)].$$

According to this numerical integration scheme, the second differential equation of the system (2.4) may be solved numerically through the discrete-time rule:

$$v_{k+1} = \overset{\mathbb{G}}{\mathrm{P}}^{x_k \to x_{k+1}}[v_k + h(-(\mathbb{G}^\sharp_{x_k} \circ \mathrm{d}_{x_k})V_x + \mathbb{G}^\sharp_{x_k}(f_x))]. \tag{3.2}$$

Note that the Christoffel term is not necessary anymore because the numerical solver ensures the vector v_{k+1} to be tangent to the manifold M at the point x_{k+1}. In the case that the manifold M is a Lie group, however, the tangent bundle is trivial, therefore parallel transport is no longer required to solve the differential equation on the variable v, as it will be illustrated in the following subsections.

The specific manifolds recalled in the following subsections, of particular interest in applications, are the Stiefel manifold, the special orthogonal group, the unit hypersphere and the manifold of symmetric positive-definite matrices.

3.1. Discrete-time second-order autonomous oscillators on the unit-hypersphere. The unit hypersphere is defined as $\mathrm{S}^{n-1} \overset{\mathrm{def}}{=} \left\{x \in \mathbb{R}^n | x^T x = 1\right\}$. A number of algorithms insist on the manifold S^{n-1}, as in blind deconvolution [12], robust constrained beamforming [10] and antennas arrays design [18].

For the unit-hypersphere endowed with the canonical metric $\mathbb{G}_x(w,v) = w^T v$, it holds that:

$$\left\{ \begin{array}{l} \overset{\mathbb{G}}{\Gamma}_x(v,v) = x\|v\|^2, \\ \overset{\mathbb{G}}{\mathrm{P}}^{x \to y}(w) = \left[I_n - \frac{(I_n - xx^T)yy^T}{1+x^T y} - xy^T\right] w, \end{array} \right. \tag{3.3}$$

where the symbol $\|\cdot\|$ denotes the vector 2-norm, the symbol I_n denotes a $n \times n$ identity matrix, $x \in \mathrm{S}^{n-1}$, $w, v \in T_x\mathrm{S}^{n-1}$. It is assumed that $x^T y \neq -1$ in the expression of the parallel transport.

For the unit-hypersphere endowed with the canonical metric, the squared Riemannian distance between two sufficiently-close points $x, y \in \mathrm{S}^{n-1}$ may be expressed in closed form as:

$$d^2(x,y) = \arccos^2(x^T y). \tag{3.4}$$

Likewise, the exponential map and its inverse, the logarithmic map, may be expressed in closed form as:

$$\left\{ \begin{array}{l} \exp_x(v) = x\cos(\|v\|) + v\,\mathrm{sinc}\,(\|v\|), \\ \log_x(y) = (I_n - xx^T)y(\mathrm{sinc}\,d(x,y))^{-1}. \end{array} \right. \tag{3.5}$$

In the expression of the exponential, it is assumed that $v \neq 0$

Whenever the p.e.f. V_x is not written in terms of the Riemannian distance function but as a plain function of the vector-variable x (as, for instance, the quadratic potential $V_x = \frac{1}{2}x^T S x$), its Riemannian gradient may be computed via the expression:

$$\mathbb{G}^\sharp_x(\mathrm{d}_x V_x) = (I_n - xx^T)\partial_x V_x. \tag{3.6}$$

By gathering the Christoffel operator and the Riemannian gradient of the p.e.f., the following nonlinear oscillator is obtained:

$$\left\{ \begin{array}{rcl} \dot{x} &=& v, \\ \dot{v} &=& -\|v\|^2 x - (I_n - xx^T)\partial_x V_x - \mu\|v\|^{2(\epsilon-1)}v - \varphi_x(v), \end{array} \right. \tag{3.7}$$

where $x(0) = x_0 \in \mathrm{S}^{n-1}$, $v(0) = v_0 \in T_{x_0}\mathrm{S}^{n-1}$ and $\varphi_x : T_x\mathrm{S}^{n-1} \to T_x\mathrm{S}^{n-1}$.

According to the expressions of the geometric quantities of interest recalled above, the discrete-time version of the dynamical system (3.7) reads:

$$\left\{ \begin{array}{rcl} x_{k+1} &=& x_k\cos(h\|v_k\|) + h\,v_k\,\mathrm{sinc}\,(h\|v_k\|), \\ v_{k+1} &=& \overset{\mathbb{G}}{\mathrm{P}}^{x_k \to x_{k+1}}[v_k - h\mu\|v_k\|^{2(\epsilon-1)}v_k - h\varphi_{x_k}(v_k) - h(I_n - x_k x_k^T)\partial_{x_k} V_x], \end{array} \right. \tag{3.8}$$

with $h > 0$ being a discretization stepsize for the dynamical system and $k = 0, 1, 2, \ldots$. Note that the Christoffel term is a normal component and hence it was taken out from the equations. The system state is represented by the variable-pair $(x_k, v_k) \in T\mathrm{S}^{n-1}$ for any $k \in \mathbb{N}$.

3.2. Discrete-time second-order autonomous oscillators on the manifold of special orthogonal matrices. The manifold of special orthogonal matrices (namely, of the multi-dimensional rotations) is defined as $\mathrm{SO}(n) \stackrel{\text{def}}{=} \left\{x \in \mathbb{R}^{n\times n} | x^T x = I_n,\ \det(x) = 1\right\}$. The tangent spaces exhibit the structure $T_x\mathrm{SO}(n) = \{x\omega | \omega \in \mathfrak{so}(n)\}$, where $\mathfrak{so}(n) \stackrel{\text{def}}{=} \{\omega \in \mathbb{R}^{n\times n} | \omega^T + \omega = 0\}$. A number of applications deal with special orthogonal matrices as invariant visual perception [32] and blind source separation [20]. (For a review of other applications, readers might want to see, e.g., [11].)

The tangent bundle $T\mathrm{SO}(n)$ may be trivialized as $\mathrm{SO}(n) \times \mathfrak{so}(n)$. The Christoffel operator associated with the special orthogonal group endowed with the canonical metric $\mathbb{G}_x(w, v) = \mathrm{tr}(w^T v)$, reads:

$$\stackrel{\mathbb{G}}{\Gamma}_x(x\omega, x\omega) = -x\omega^2, \tag{3.9}$$

where $x \in \mathrm{SO}(n)$, $\omega \in \mathfrak{so}(n)$.

For the special orthogonal group endowed with the canonical metric, the exponential map and the logarithmic map may be expressed in closed form as:

$$\left\{\begin{array}{l} \exp_x(v) = x\mathrm{Exp}(x^T v), \\ \log_x(y) = x\mathrm{Log}(x^T y), \end{array}\right. \tag{3.10}$$

where $x, y \in \mathrm{SO}(n)$, $w, v \in T_x\mathrm{SO}(n)$, the symbols 'Exp' and 'Log' denote the matrix exponential and the principal matrix logarithm, respectively.

The squared Riemannian distance between two sufficiently-close points $x, y \in \mathrm{SO}(n)$ may be expressed in closed form as:

$$d^2(x, y) = -\mathrm{tr}(\mathrm{Log}^2(x^T y)), \tag{3.11}$$

where the symbol 'tr' denotes matrix trace. (Note that the skew-symmetric matrix $\mathrm{Log}(x^T y)$ is semidefinite-negative, hence $-\mathrm{tr}(\mathrm{Log}^2(x^T y)) \geq 0$.)

Whenever the p.e.f. V_x is written as a plain function of the matrix-variable x (as, for instance, the quadratic potential $V_x = \frac{1}{2}\mathrm{tr}(x^T S x)$), its Riemannian gradient may be computed via the expression:

$$\mathbb{G}_x^\sharp(\mathrm{d}_x V_x) = \tfrac{1}{2}\left(\partial_x V_x - x\partial_x^T V_x x\right). \tag{3.12}$$

Straightforward calculations lead to the dynamics:

$$\left\{\begin{array}{rcl} \dot{x} &=& x\omega, \\ \dot{\omega} &=& -\frac{1}{2}\left(x^T\partial_x V_x - \partial_x^T V_x x\right) - \mu\|\omega\|^{2(\epsilon-1)}\omega - \tilde{\varphi}_x(\omega), \end{array}\right. \tag{3.13}$$

with $x(0) = x_0 \in \mathrm{SO}(n)$ and $\omega(0) = \omega_0 \in \mathfrak{so}(n)$. In the present context, $\tilde{\varphi}_x$ is a $\mathfrak{so}(n)$-algebra endomorphism.

The system (3.13) may be implemented numerically as:

$$\left\{\begin{array}{rcl} x_{k+1} &=& x_k\mathrm{Exp}(h\, x_k\omega_k), \\ \omega_{k+1} &=& \frac{1}{2}h\left(\partial_{x_k}^T V_x x_k - x_k^T\partial_{x_k} V_x\right) + (1 - h\mu\|\omega_k\|^{2(\epsilon-1)})\omega_k - h\tilde{\varphi}_{x_k}(\omega_k), \end{array}\right. \tag{3.14}$$

where $h > 0$ plays the role of a discretization stepsize for the dynamical system. The system state is represented by the pair $(x_k, \omega_k) \in \mathrm{SO}(n) \times \mathfrak{so}(n)$ for $k \in \mathbb{N}$. The first equation of the numerical method (3.14) represents a geodesic-based step-forward numerical approximation of the flow associated with the first differential equation on the tangent bundle $T\mathrm{SO}(n)$. The second equation represents a direct Euler-like step-forward method that can be implemented as is because the flow of the second differential equation of the system (3.13) takes place on a single linear space, namely, the Lie algebra $\mathfrak{so}(n)$.

3.3. Discrete-time second-order autonomous oscillators on the manifold of symmetric, positive-definite matrices. The manifold of symmetric, positive-definite matrices is defined as $\mathrm{S}^+(n) \stackrel{\text{def}}{=} \{x \in \mathbb{R}^{n\times n} | x^T - x = 0,\ x > 0\}$. The tangent bundle exhibits a trivial structure as $T_x\mathrm{S}^+(n) = \mathrm{S}(n) \stackrel{\text{def}}{=} \{v \in \mathbb{R}^{n\times n} | v^T - v = 0\}$ for every $x \in \mathrm{S}^+(n)$. Symmetric positive-definite matrices are used in the analysis of deformations [31], in pattern recognition [17], in cognitive computation [14] and in computational neurology [4].

Since $\mathrm{S}^+(n)$ is a Lie group[1], its tangent bundle $T\mathrm{S}^+(n)$ may be trivialized as $\mathrm{S}^+(n) \times \mathrm{S}(n)$. The Christoffel operator associated with the manifold of symmetric, positive-definite matrices endowed with the canonical metric $\mathbb{G}_x(w, v) = \mathrm{tr}(x^{-1}wx^{-1}v)$, reads:

$$\overset{\mathbb{G}}{\Gamma}_x(v, v) = -vx^{-1}v, \tag{3.15}$$

with $x \in \mathrm{S}^+(n)$ and $w, v \in T_x\mathrm{S}^+(n)$.

The exponential map and the logarithmic map may be expressed in closed form as:

$$\begin{cases} \exp_x(v) = \sqrt{x}\,\mathrm{Exp}\left(\sqrt{x^{-1}}v\sqrt{x^{-1}}\right)\sqrt{x}, \\ \log_x(y) = \sqrt{x}\,\mathrm{Log}\left(\sqrt{x^{-1}}y\sqrt{x^{-1}}\right)\sqrt{x}. \end{cases} \tag{3.16}$$

where $x \in \mathrm{S}^+(n)$ and $v \in T_x\mathrm{S}^+(n)$, while the symbol $\sqrt{\cdot}$ denotes symmetric matrix square root.

According with the structure of the logarithmic map, the squared Riemannian distance between two symmetric, positive-definite matrices $x, y \in \mathrm{S}^+(n)$ takes the expression:

$$d^2(x, y) = \mathrm{tr}\left(\mathrm{Log}^2\left(\sqrt{x^{-1}}y\sqrt{x^{-1}}\right)\right). \tag{3.17}$$

Whenever the p.e.f. V_x is written as a plain function of the matrix-variable x, its Riemannian gradient may be computed via the expression:

$$\mathbb{G}^\sharp_x(\mathrm{d}_x V_x) = \tfrac{1}{2}x\left(\partial_x V_x + \partial_x^T V_x\right)x. \tag{3.18}$$

In several interesting applications, such as in the classification of covariance matrices for brain-computer interfacing, the potential energy is a function of the Riemannian distance (see, for instance, the contribution [41]).

By gathering the expressions of the Christoffel operator and of the Riemannian gradient of the potential energy function, the following dynamical system equations are obtained:

$$\begin{cases} \dot{x} &= v, \\ \dot{v} &= vx^{-1}v - \tfrac{1}{2}x\left(\partial_x^T V_x + \partial_x V_x\right)x - \mu\|v\|_x^{2(\epsilon-1)}v - \tilde{\varphi}_x(v). \end{cases} \tag{3.19}$$

In the present case, $\tilde{\varphi} : \mathrm{S}^+(n) \times \mathrm{S}(n) \to \mathrm{S}(n)$. The system (3.19) may be implemented numerically as:

$$\begin{cases} x_{k+1} &= \sqrt{x_k}\,\mathrm{Exp}\left(h\sqrt{x_k^{-1}}v_k\sqrt{x_k^{-1}}\right)\sqrt{x_k}, \\ v_{k+1} &= h\left[-\tfrac{1}{2}x_k(\partial_{x_k}^T V_x + \partial_{x_k} V_x)x_k\right] + (1 - h\mu\|v\|_{x_k}^{2(\epsilon-1)})v_k - h\tilde{\varphi}_{x_k}(v_k), \end{cases} \tag{3.20}$$

where $h > 0$ plays the role of a discretization stepsize for the nonlinear oscillator and $k = 0, 1, 2, \ldots$. In this case, the system state is represented by the pair $(x_k, v_k) \in \mathrm{S}^+(n) \times \mathrm{S}(n)$ for $k \in \mathbb{N}$.

[1] We recall that the space $\mathrm{S}^+(n)$ is not an algebraic group with respect to the standard matrix multiplication (namely, given two matrices $x_1, x_2 \in \mathrm{S}^+(n)$, their standard matrix product $x_1 \cdot x_2$ is, in general, not symmetric). However, it can be made an algebraic group with respect to a "modified" multiplication, namely $x_1 \odot x_2 \stackrel{\text{def}}{=} \mathrm{Exp}(\mathrm{Log}(x_1) + \mathrm{Log}(x_2))$ for any $x_1, x_2 \in \mathrm{S}^+(n)$. The group identity, in this setting, is the unit matrix I_n (in fact $x_1 \odot I_n = I_n \odot x_1 = x_1$) and the group inversion is the standard matrix inversion (which may be rewritten as $x_1^{-1} = \mathrm{Exp}(-\mathrm{Log}(x_1))$, that helps showing that $x_1 \odot x_1^{-1} = x_1^{-1} \odot x_1 = I_n$).

3.4. Discrete-time second-order autonomous oscillators on the compact Stiefel manifold. The compact Stiefel manifold is defined as $\mathrm{St}(n,p) \stackrel{\text{def}}{=} \{x \in \mathbb{R}^{n\times p} | x^T x = I_p\}$, where $p \leq n$. The tangent spaces to the Stiefel manifold exhibit the structure $T_x\mathrm{St}(n,p) \stackrel{\text{def}}{=} \{v \in \mathbb{R}^{n\times p} | x^T v + v^T x = 0\}$. Exemplary applications where the compact Stiefel manifold plays a prominent role are non-negative matrix factorization [48], direction of arrival estimation [23], electronic structures computation [7] and factor analysis in psychometrics [8]. For the Stiefel manifold, some quantities of interest are not available in closed form in the scientific literature, hence, a specific discrete-time version of the oscillator equations need to be devised.

When the Stiefel manifold is endowed with its canonical metric

$$\mathbb{G}_x(w,v) = \mathrm{tr}\left(w^T v\right) - \tfrac{1}{2}\mathrm{tr}\left(w^T x x^T v\right), \tag{3.21}$$

the following geometric characterization holds:

$$\left\{\begin{array}{l} \overset{\mathbb{G}}{\Gamma}_x(v,v) = -vv^T x - xv^T(I_n - xx^T)v, \\ \exp_x(v) = [x\ q]\mathrm{Exp}\left(\left[\begin{array}{cc} x^T v & -r^T \\ r & 0_p \end{array}\right]\right)\left[\begin{array}{c} I_p \\ 0_p \end{array}\right], \\ \mathbb{G}^\sharp_x(\mathrm{d}_x V_x) = \partial_x V_x - x\partial_x^T V_x x, \\ \overset{\mathbb{G}}{\mathrm{P}}{}^{0\to t}_{\gamma_{x,v}}(v) = [v\ -xr^T]\mathrm{Exp}\left(t\left[\begin{array}{cc} x^T v & -r^T \\ r & 0_p \end{array}\right]\right)\left[\begin{array}{c} I_p \\ 0_p \end{array}\right], \end{array}\right. \tag{3.22}$$

where q and r denote the factors of the compact QR decomposition of the matrix $(I_n - xx^T)v$ and 0_p denotes a zero $p \times p$ matrix. Note that, for the Stiefel manifold endowed with the canonical metric, to the best of the author's knowledge, the expression of the Riemannian distance $d(\cdot,\cdot)$, of the general parallel transport operation and of the logarithmic map are unknown[2]. Hence, the equations (3.22) were developed by making use of the parallel transport of the initial tangent vector along its own geodesic only.

By the expressions of the Riemannian gradient of the potential energy function and of the Christoffel form, the following dynamical system is obtained:

$$\left\{\begin{array}{rcl} \dot{x} &=& v, \\ \dot{v} &=& vv^T x + xv^T(I_n - xx^T)v - (\partial_x V_x - x\partial_x^T V_x x) - \mu\|v\|_x^{2(\epsilon-1)} v - \varphi_x(v), \end{array}\right. \tag{3.23}$$

where $\varphi : T\mathrm{St}(n,p)\mathbb{R} \to T\mathrm{St}(n,p)$.

According to the expression of the geodesic on the Stiefel manifold endowed with the canonical metrics and of the self-parallel-transport formula corresponding to the canonical metrics, the dynamical system (3.23) may be implemented as:

$$\left\{\begin{array}{lcl} a_k &\stackrel{\text{def}}{=}& (1 - h\mu\|v_k\|_{x_k}^{2(\epsilon-1)})v_k - h\varphi_{x_k}(v_k) - h\left(\partial_{x_k} V - x_k(\partial_{x_k} V)^T x_k\right), \\ (q_k, r_k) &\stackrel{\text{def}}{=}& \mathrm{cqr}((I_n - x_k x_k^T)a_k), \\ E_k &\stackrel{\text{def}}{=}& \mathrm{Exp}\left(h\left[\begin{array}{cc} x_k^T a_k & -r_k^T \\ r_k & 0_p \end{array}\right]\right)\left[\begin{array}{c} I_p \\ 0_p \end{array}\right], \\ x_{k+1} &=& [x_k\ q_k]E_k, \\ v_{k+1} &=& [a_k\ -x_k r_k^T]E_k, \end{array}\right. \tag{3.24}$$

where $h > 0$ is a stepsize for the nonlinear oscillator, $\mathrm{cqr}(\cdot)$ denotes the compact QR factorization operator and $k = 0, 1, 2, \ldots$. The system state is represented by the pair $(x_k, v_k) \in T\mathrm{St}(n,p)$ for $k \in \mathbb{N}$.

[2]It might be interesting to the practitioners to know that there exists an iterative algorithm that is able to compute, only numerically and approximately, the logarithmic map (and hence the distance) of two Stiefel matrices (provided that these matrices do not lay too far from one another). The algorithm and the related computer code are publicly available [50]).

3.5. Discussion on energy conservation. For the sake of notation conciseness, the discrete-time, nonlinear oscillator equations are rewritten here as in the Section 3, namely:

$$\left\{ \begin{array}{l} x_{k+1} = \exp_{x_k}(h\, v_k), \\ v_{k+1} = \overset{\mathbb{G}}{\mathrm{P}}{}^{x_k \to x_{k+1}}[v_k + h\, F(x_k)], \end{array} \right. \tag{3.25}$$

where it is assumed that the forcing term $F : M \to TM$ stems from a potential energy function only, namely, $F(x_k) = -\mathbb{G}^{\sharp}_{x_k}(\mathrm{d}_{x_k} V_x)$. Recall that the parallel transport operator is linear in its argument (although it is markedly nonlinear in the quantities x_k and x_{k+1}), therefore, the second equation may be written equivalently as:

$$v_{k+1} = \overset{\mathbb{G}}{\mathrm{P}}{}^{x_k \to x_{k+1}}(v_k) + h\, \overset{\mathbb{G}}{\mathrm{P}}{}^{x_k \to x_{k+1}}[F(x_k)]. \tag{3.26}$$

For a conservative oscillator, it was recalled in the Subsection 2.2 that the total energy $H_x = K_x + V_x$ keeps constant over time. The present subsection aims at investigating whether such property is retained when passing from the continuos-time equations to the discrete-time equations. The total energy at the discrete-time k takes the value:

$$H_{x_k} = V_{x_k} + \tfrac{1}{2}\mathbb{G}_{x_k}(v_k, v_k). \tag{3.27}$$

The total energy at the discrete-time $k+1$ takes the value:

$$H_{x_{k+1}} = V_{x_{k+1}} + \tfrac{1}{2}\mathbb{G}_{x_{k+1}}(v_{k+1}, v_{k+1}). \tag{3.28}$$

Since the inner product $\mathbb{G}_{\cdot}(\cdot,\cdot)$ is bilinear, plugging the right-hand side of the equation (3.26) into the above relationship yields:

$$\begin{aligned} H_{x_{k+1}} = {} & V_{x_{k+1}} \\ & + \tfrac{1}{2}\mathbb{G}_{x_{k+1}}(\overset{\mathbb{G}}{\mathrm{P}}{}^{x_k \to x_{k+1}}(v_k), \overset{\mathbb{G}}{\mathrm{P}}{}^{x_k \to x_{k+1}}(v_k)) \\ & + \tfrac{1}{2}h^2\mathbb{G}_{x_{k+1}}(\overset{\mathbb{G}}{\mathrm{P}}{}^{x_k \to x_{k+1}}[F(x_k)], \overset{\mathbb{G}}{\mathrm{P}}{}^{x_k \to x_{k+1}}[F(x_k)]) \\ & + h\mathbb{G}_{x_{k+1}}(\overset{\mathbb{G}}{\mathrm{P}}{}^{x_k \to x_{k+1}}(v_k), \overset{\mathbb{G}}{\mathrm{P}}{}^{x_k \to x_{k+1}}[F(x_k)]). \end{aligned} \tag{3.29}$$

Recall that the parallel transport is an isometry, namely, it preserves the inner product with respect to the metric $\mathbb{G}$, hence:

$$H_{x_{k+1}} = V_{x_{k+1}} + \tfrac{1}{2}\mathbb{G}_{x_k}(v_k, v_k) + \tfrac{1}{2}h^2\mathbb{G}_{x_k}(F(x_k), F(x_k)) + h\mathbb{G}_{x_k}(v_k, F(x_k)).$$

As a consequence, the total energy at the discrete-time $k+1$ may be written, in terms of the total energy at the discrete-time k, as:

$$H_{x_{k+1}} - H_{x_k} = V_{x_{k+1}} - V_{x_k} + \tfrac{1}{2}h^2\|F(x_k)\|^2_{x_k} + h\mathbb{G}_{x_k}(v_k, F(x_k)).$$

Although, when $h \to 0$, the difference $H_{x_{k+1}} - H_{x_k} \to 0$ because $x_{k+1} \to x_k$, for h finite, the conclusion is that, upon time-discretization of the continuos-time equations, the energy conservation property does not replicate. It is worth underlying that, if an oscillator is designed with the purpose of producing a reference signal independently of any physical phenomena, the lack of energy conservation may be ignored. Numerical simulations suggested that, in cases of interest, the two terms $\frac{1}{2}h^2\|F(x_k)\|^2_{x_k} + h\mathbb{G}_{x_k}(v_k, F(x_k))$ combine in a way that *increases* the total energy of the system: in such event, the unwanted (albeit slow) increase of energy may be countered by an additional dissipative term, such as the one corresponding to Rayleigh damping.

4. Examples. The current section presents two examples based on the manifold S^2, in order to illustrate the potential of the devised nonlinear damped oscillators on manifold. The ordinary sphere S^2 was chosen because it affords graphical rendering. (The MATLAB© codes are available on request.)

4.1. A Lorenz-like oscillator on the sphere. The Lorenz oscillator is a classical nonlinear dynamical system described by the equations:

$$\left\{ \begin{array}{rcl} \dot{z} &=& w, \\ \dot{w} &=& -[A + B(z)]w, \end{array} \right. \tag{4.1}$$

where the state $z = [z_1,\ z_2,\ z_3]^T \in \mathbb{R}^3$ and

$$A \stackrel{\text{def}}{=} \left[\begin{array}{ccc} \sigma & -\sigma & 0 \\ -\rho & 1 & 0 \\ 0 & 0 & \beta \end{array} \right],\ B(z) \stackrel{\text{def}}{=} \left[\begin{array}{ccc} 0 & 0 & 0 \\ z_3 & 0 & z_1 \\ -z_2 & -z_1 & 0 \end{array} \right]. \tag{4.2}$$

(Initial conditions omitted.) For certain values of the parameters $\sigma, \rho, \beta > 0$, the system exhibits a complex behavior. Setting $x(t) = z(t)\|z(t)\|^{-1}$ and deriving twice with respect to the temporal parameter t leads to a version of the Lorenz oscillator on the sphere S^2 (see the Appendix A for the detailed calculations). Such a dynamical system appears as a special case of the general system on the sphere (3.7) and reads:

$$\left\{ \begin{array}{rcl} \dot{x} &=& v, \\ \dot{v} &=& -\|v\|^2 x - 2\lambda v - \varphi_x(v), \end{array} \right. \tag{4.3}$$

where $x(0) = x_0 \in \mathrm{S}^2$, $v(0) = v_0 \in T_{x_0}\mathrm{S}^2$, and

$$\varphi_x(v) = (I_3 - xx^T)[A + \nu B(x)](v + \lambda x), \tag{4.4}$$

with A and B defined as in (4.2) and $\nu, \lambda \in \mathbb{R}$ being constant parameters.

The above autonomous, damped oscillator was implemented by the discrete-time rule (3.8), namely:

$$\left\{ \begin{array}{rcl} x_{k+1} &=& x_k \cos(h\|v_k\|) + h\, v_k\, \mathrm{sinc}\,(h\|v_k\|), \\ v_{k+1} &=& (1 - 2h\lambda) \overset{\mathbb{G}}{\mathrm{P}}{}^{x_k \to x_{k+1}}(v_k) - h \overset{\mathbb{G}}{\mathrm{P}}{}^{x_k \to x_{k+1}}[\varphi_{x_k}(v_k)], \end{array} \right.$$

with $h = \frac{3}{500}$ and $k = 0, 1, 2, \ldots, 5000$. The Figure 4.1 illustrates a trajectory obtained by initializing x_0 randomly on the sphere, v_0 randomly in the tangent space $T_{x_0}\mathrm{S}^2$, with the classical values of the Lorenz parameters $\rho = 28$, $\sigma = 10$, $\beta = \frac{8}{3}$ and with the specific parameters of the Lorenz-like oscillator on the sphere set to $\nu = 400$ and $\lambda = 2$ (since $2h\lambda \ll 1$, the approximation $1 - 2h\lambda \approx 1$ was used in the code). From the Figure 4.1, the complex non-repeating shape of the trajectory generated by the oscillator over the surface of the base-manifold may be appreciated. The shape of the trajectory varies greatly when varying the values of the parameters and the initial conditions.

4.2. An oscillator on the sphere based on a quadratic potential. A special case of the general autonomous, damped oscillator on the sphere (3.7) is:

$$\left\{ \begin{array}{rcl} \dot{x} &=& v, \\ \dot{v} &=& -\|v\|^2 x - \mu\|v\|v - (I_3 - xx^T)Sx, \end{array} \right. \tag{4.5}$$

where $x(0) = x_0 \in \mathrm{S}^2$, $v(0) = v_0 \in T_{x_0}\mathrm{S}^2$ and $S \in \mathrm{S}^+(3)$. The above oscillator corresponds to a quadratic p.e.f. $V_x = \frac{1}{2}x^T Sx$ and to a generalized Rayleigh damping term with damping exponent $\epsilon = \frac{3}{2}$.

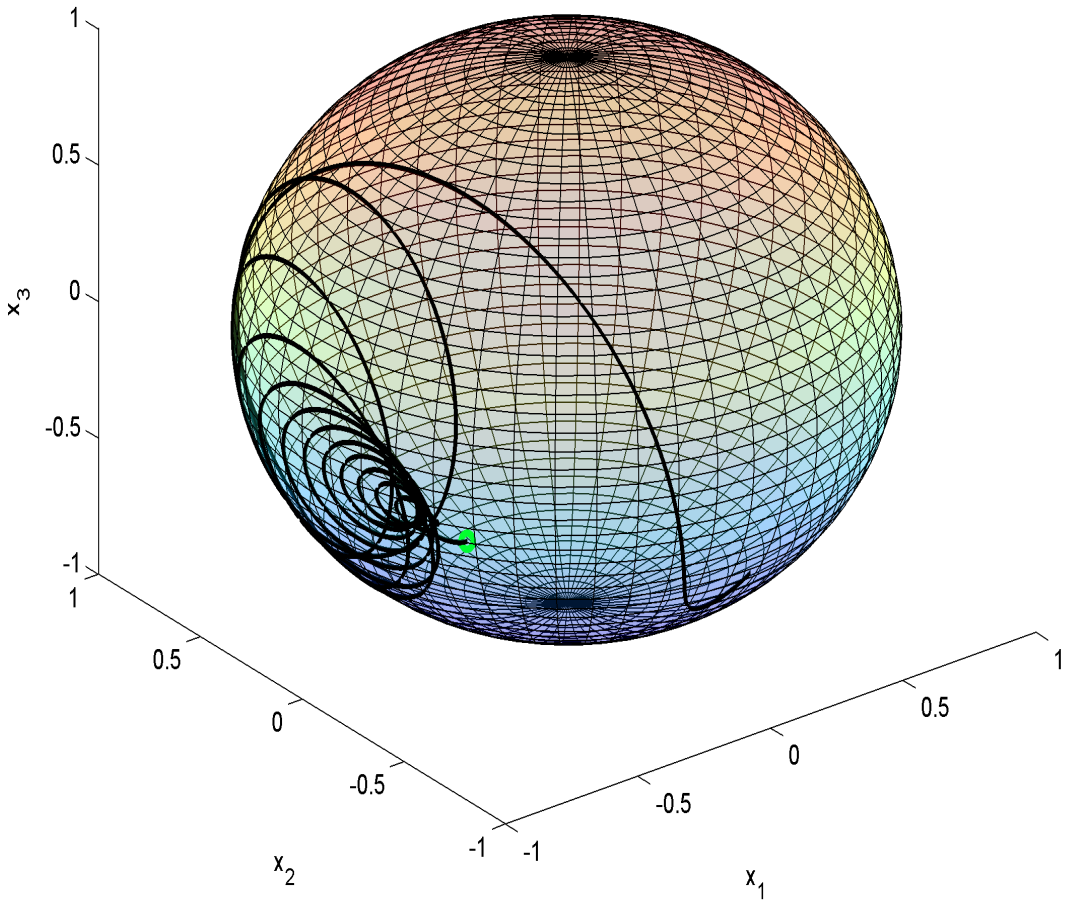

FIG. 4.1. *Oscillatory dynamics on the manifold $M = \mathrm{S}^2$ of the dynamical system (4.3)+(4.4). Trajectory over the unit sphere: The circle denotes the initial point.*

The above autonomous, damped oscillator was implemented by the discrete-time rule:

$$\left\{ \begin{array}{rcl} x_{k+1} & = & x_k \cos(h\|v_k\|) + h\, v_k \,\mathrm{sinc}\,(h\|v_k\|), \\ v_{k+1} & = & \overset{\mathbb{G}}{\mathrm{P}}{}^{x_k \to x_{k+1}}(v_k) - h \overset{\mathbb{G}}{\mathrm{P}}{}^{x_k \to x_{k+1}}[\mu\|v_k\| v_k + (I_3 - x_k x_k^T) S x_k], \end{array} \right. \tag{4.6}$$

with $h = \frac{1}{100}$ and $k = 0, 1, 2, \ldots, 5000$. The Figure 4.2 illustrates a trajectory obtained by initializing x_0 randomly on the sphere, v_0 randomly in the tangent space $T_{x_0}\mathrm{S}^2$, S randomly in $\mathrm{S}^+(3)$ and $\mu = \frac{1}{100}$ (as suggested in the Subsection 3.5, the passive damping has the purpose of stabilizing the dynamics against

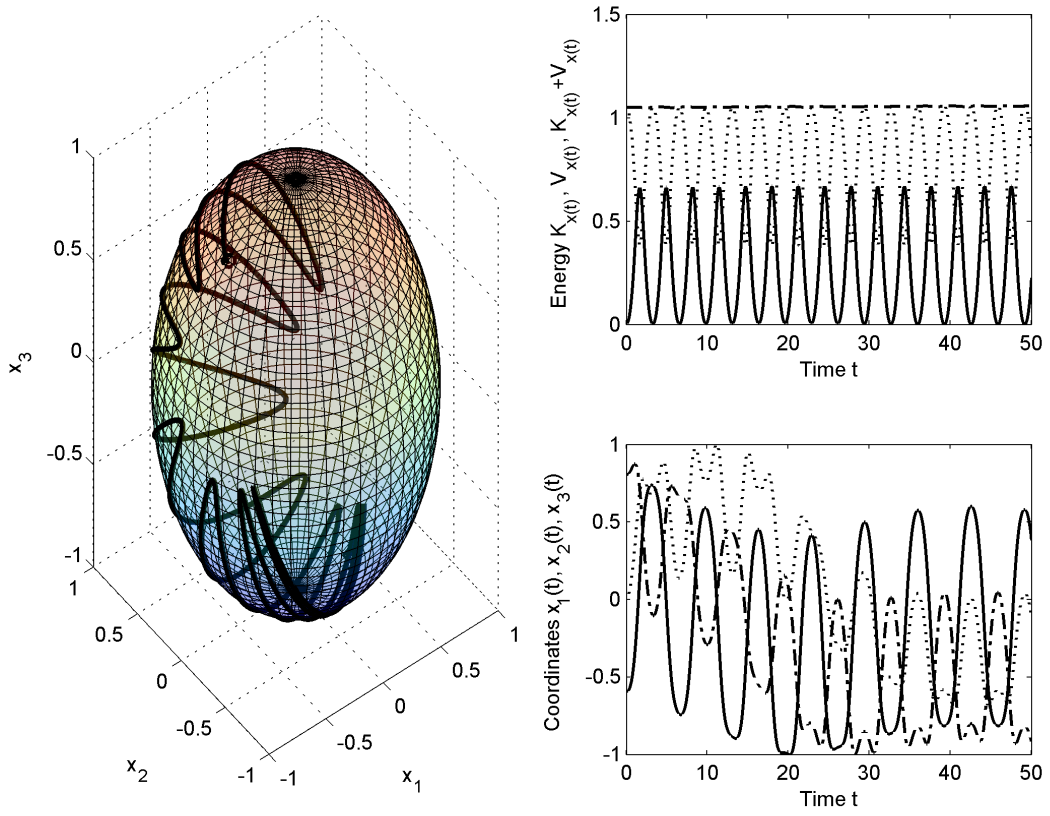

FIG. 4.2. *Oscillatory dynamics on the manifold $M = \mathrm{S}^2$, embedded in the Euclidean space $\mathbb{R}^3$, of the system (4.6). The p.e.f. is $V_x = \frac{1}{2}x^T Sx$, with S random, symmetric, positive-definite. The left-hand panel illustrates the trajectory over the sphere (the circle denotes the initial point). The upper panel on the right-hand side illustrates the values of the kinetic energy K_x (solid line), the potential energy V_x (dotted line) and the total energy H_x (dot-dashed line) over the trajectory. The lower panel on the right-hand side illustrates the trajectory in terms of the three embedded coordinates x_1, x_2, x_3.*

a growth of its Hamiltonian induced by the time discretization). From the Figure 4.2, it is appreciated how, after a transient phase, the system enters a limit cycle and generates a periodic trajectory over the base-manifold. The total energy keeps almost constant over the whole trajectory, confirming that the generalized Rayleigh damping term is able to counter the slow "energy drift" caused by the numerical integration method.

5. Conclusion. The purpose of the present contribution was to describe a general second-order, autonomous, damped oscillator model on Riemannian manifolds. Starting from a formulation available in continuous time [15], we developed discrete-time equations and particularized them to manifolds of interest in sciences and engineering, such as the hyper-sphere and the space of the symmetric, positive-definite matrices. Computer simulations served to illustrate the numerical behavior of the devised model.

The present paper aimed at presenting some fundamental notions and properties of non-linear, possibly chaotic, oscillators on Riemannian manifolds, which might be applied to solving scientific and engineering problems in the future. Two of such possible employments are:

- *Possible application to the optimization of complex functions*: The global optimization of com-

plex, multi-variables, possibly non-differentiable functions is an involved and challenging problem encountered in diverse fields of applications. Since a non-linear oscillator may produce a chaotic motion that traverses non-repeatedly a certain search domain, by making use of the known properties of chaos, an effective optimization method was proposed in the recent past, namely, the Chaos-based Optimization Algorithm (COA, [3], see, e.g., [42] for a comprehensive review). This optimization technique may now be extended to the optimization of non-smooth functions on Riemannian manifolds. It is to be noted how the chaos-based optimization method works by two subsequent stages, termed 'waves': The first wave performs a broad search within the feasible space and determines a first (sub-optimal) solution, while the second wave is meant to perform a fine search in a neighborhood of the provisional sub-optimal solution. Such two-stage search suggests the need of two kinds of oscillatory behaviors: local (i.e., limited to a specific volume of the feasible manifold) and global (i.e., potentially able to explore the whole manifold volume).

- *Possible application to encryption for the secure transmission of information*: Encryption of important information benefits from chaotic oscillators, in that chaotic signals improve the security of the encrypted data (and, as a by-product, it might result in a significant data compression, see [28]). The resulting high-security architectures are ideal in a number of real-life applications such as the transmission and storage of medical images and of legal documents. In general, non-linear oscillators are the inner engines of such secure communication systems, where the variables generated by the oscillators are used to mask information signals [47]. These systems may now be extended to masking and encrypting structured (i.e., manifold-valued) signals as well as multiple real-valued (or complex-valued) signals.

On the theoretical side, there are two foreseen future steps to be taken along the present research thread, namely:

- *Development of more sophisticated numerical integration techniques*: The numerical integration technique used within the present paper is a forward Euler scheme adapted to curved spaces by means of appropriate differential-geometrical tools. There exist further schemes in the literature of numerical calculus that might be implemented instead, such as the backward Euler method, the "trapezoidal" method, the Cavalieri-Simpson rule and the Newton-Cotes rule. Some of these methods are potentially more accurate than the forward Euler method but also more burdensome from a computational point of view, therefore, the forward Euler method was chosen in this paper as a good trade-off between numerical accuracy and computational ease. In future research endeavors, it will be interesting to extend some of the above methods to curved manifolds and, in particular, the Runge-Kutta scheme, which is particularly popular in engineering and applied sciences: see, for example, the paper [49] which still covers the Euclidean (non-curved) case.
- *Development of synchronization techniques*: The temporal synchronization of two oscillators of the same type (for example, two Lorenz-like oscillators), insisting on the same manifold as state space, seems of prime importance in the secure transmission of information (see, for example, the contribution [47]). Temporal synchronization is a well-studied problem in the Euclidean setting and its extension to curved spaces appears as a challenging scientific endeavor. The extension of a control-theoretic synchronization method based on the Lyapunov stability theory (commonly referred to in systems theory as *pinning control scheme*) to first-order and second-order dynamical systems on manifolds is currently under investigation by the present author.

Acknowledgments. The present research was partially financed by the uPM grant *Ricerca Scientifica di Ateneo RSA-2014 - Parte B*. The author wishes to express his gratitude to the anonymous Reviewers and to the Editors for the excellent quality and insight level of their review reports.

REFERENCES

[1] A. Ciaramella, E. De Lauro, S. De Martino, B. Di Lieto, M. Falanga and R. Tagliaferri, *Characterization of Strombolian events by using independent component analysis*, Nonlinear Processes in Geophysics, Vol. 11, pp. 453 – 461, 2004

[2] M. Camarinha, F. Silva Leite and P. Crouch, *On the geometry of Riemannian cubic polynomials*, Differential Geometry and Its Applications, Vol. 15, pp. 107 – 135, 2001

[3] B. Li and W. Jiang, *Optimizing complex functions by chaos search*, Cybernetics and Systems: An International Journal, Vol. 29, No. 4, pp. 409 – 419, 1998

[4] P. Chossat and O. Faugeras, *Hyperbolic planforms in relation to visual edges and textures perception*, PLoS Computational Biology. DOI: 10.1371/journal.pcbi.1000625, 2009

[5] D.-I. Curiac and C. Volosencu, *A 2D chaotic path planning for mobile robots accomplishing boundary surveillance missions in adversarial conditions*, Communications in Nonlinear Science and Numerical Simulation, Vol. 19, No. 10, pp 3617 – 3627, October 2014

[6] W. Ditto and T. Munakata, *Principles and applications of chaotic systems*, Communications of the ACM, Vol. 38, No. 11, pp. 96 – 102, November 1995

[7] A. Edelman, T.A. Arias and S.T. Smith, *The geometry of algorithms with orthogonality constraints*, SIAM Journal on Matrix Analysis Applications, Vol. 20, No. 2, pp. 303 – 353, 1998

[8] L. Eldén and H. Park, *A Procrustes problem on the Stiefel manifold*, Numerical Mathematics, Vol. 82, pp. 599 – 619, 1999

[9] B. Esser and D. Huston, *Active mass damping of electronic circuit boards*, Journal of Sound and Vibration, Vol. 277, No. 1-2, pp. 419 – 428, October 2004

[10] S. Fiori, *Neural minor component analysis approach to robust constrained beamforming*, IEE Proceedings – Vision, Image and Signal Processing, Vol. 150, No. 4, pp. 205 – 218, August 2003

[11] S. Fiori, *Quasi-geodesic neural learning algorithms over the orthogonal group: A tutorial*, Journal of Machine Learning Research, Vol. 6, pp. 743 – 781, May 2005

[12] S. Fiori, *Geodesic-based and projection-based neural blind deconvolution algorithms*, Signal Processing, Vol. 88, No. 3, pp. 521 – 538, March 2008

[13] S. Fiori and T. Tanaka, *An Algorithm to compute averages on matrix Lie groups*, IEEE Transactions on Signal Processing, Vol. 57, No. 12, pp. 4734 – 4743, December 2009

[14] S. Fiori, *Learning the Fréchet mean over the manifold of symmetric positive-definite matrices*, Cognitive Computation, Vol. 1, No. 4, pp. 279 – 291, December 2009

[15] S. Fiori, *Nonlinear damped oscillators on Riemannian manifolds: Fundamentals*, Journal of Systems Science and Complexity, Vol. 29, No. 1, pp. 22 – 40, February 2016

[16] R. FitzHugh, *Mathematical models of excitation and propagation in nerve*, in "Biological Engineering" (H.P. Schwan, ed.), pp. 1 – 85, McGraw-Hill, New York, 1969

[17] M.T. Harandi, C. Sanderson, A. Wiliem and B.C. Lovell, *Kernel analysis over Riemannian manifolds for visual recognition of actions, pedestrians and textures*, in Proc. of the 2012 IEEE Workshop on Applications of Computer Vision (WACV, Breckenridge (CO, USA), January 9-11, 2012), pp. 433 – 439, 2012

[18] R. Hunger, P. de Kerret and M. Joham, *An algorithm for maximizing a quotient of two hermitian form determinants with different exponents*, in Proc. of the International Conference on Acoustics, Speech and Signal Processing (ICASSP 2010, Dallas (TX, USA), March 2010), pp. 3346 – 3349, 2010

[19] T. Kaneko, S. Fiori and T. Tanaka, *Empirical arithmetic averaging over the compact Stiefel manifold*, IEEE Transactions on Signal Processing, Vol. 61, No. 4, pp. 883 – 894, February 2013

[20] T.-W. Lee, *Independent Component Analysis: Theory and Applications*, Kluwer Academic Publishers, September 1998

[21] G.A. Leonov and N.V. Kuznetsov, *On differences and similarities in the analysis of Lorenz, Chen, and Lu systems*, Applied Mathematics and Computation, Vol. 256, pp. 334 – 343, 2015

[22] E.N. Lorenz, *Deterministic nonperiodic flow*, Journal of the Atmospheric Sciences, Vol. 20, No. 2, pp. 130 – 141, 1963

[23] C.S. MacInnes and R.J. Vaccaro, *Tracking direction-of-arrival with invariant subspace updating*, in Proc. of the International Conference on Acoustics, Speech and Signal Processing (ICASSP 1996, May 7-10, 1996, Atlanta (GA), USA), pp. 2896 – 2899, 1996

[24] G.M. Maggio, O. De Feo and M.P. Kennedy, *Nonlinear analysis of the Colpitts oscillator and applications to design*, IEEE Transactions on Circuits Systems - Part I: Fundamental Theory and Applications, Vol. 46, No. 9, pp. 1118 – 1130, September 1999

[25] K. Modin and G. Söderlind, *Geometric integration of Hamiltonian systems perturbed by Rayleigh damping*, BIT Numerical Mathematics, Vol. 51, pp. 977 – 1007, 2011

[26] F.J. Molero, M. Lara, S. Ferrer and F. Cèspedes, *2-D Duffing oscillator: Elliptic functions from a dynamical systems point of view*, Qualitative Theory of Dynamical Systems, Vol. 12, No. 1, pp. 115 – 139, April 2013

[27] M. Pérez-Molina, J. Gil-Chica, E. Fernández-Varó, M.F. Pérez-Polo, *Steady state, oscillations and chaotic behavior of a gas inside a cylinder with a mobile piston controlled by PI and nonlinear control*, Communications in Nonlinear Science and Numerical Simulation, Vol. 36, pp. 468 – 495, July 2016

[28] B. Prasad and K. Mishra, *A combined encryption compression scheme using chaotic maps*, Cybernetics and Information Technologies, Vol. 13, No. 2, pp. 75 – 81, 2013

[29] B. van der Pol, *On relaxation-oscillations*, The London, Edinburgh and Dublin Philosophical Magazine & Journal of

Science, Vol. 2, No. 7, pp. 978 – 992, 1927
[30] M.I. Rabinovich and A.L. Fabrikant, *Stochastic self-modulation of waves in nonequilibrium media*, Soviet Physics (Journal of Experimental and Theoretical Physics), Vol. 50, p. 311, 1979
[31] I.U. Rahman, I. Drori, V.C. Stodden, D.L. Donoho and P. Schröder, *Multiscale representations for manifold-valued data*, Multiscale Modeling and Simulation, Vol. 4, No. 4, pp 1201 – 1232, 2005
[32] R.P.N. Rao and D.L. Ruderman, *Learning Lie groups for invariant visual perception*, Advances in Neural Information Processing Systems (NIPS) 11, pp. 810 – 816, 1999
[33] T. Roh, K. Bong, S. Hong, H. Cho and H.-J. Yoo, *Wearable mental-health monitoring platform with Independent Component Analysis and Nonlinear Chaotic Analysis*, in Proc. of the 34$^{\text{th}}$ Annual International Conference of the IEEE EMBS (San Diego, California USA, 28 August - 1 September, 2012), pp. 4541 – 4544, 2012
[34] M. Rosenblum, L. Cimponeriu and A. Pikovsky, *Coupled oscillators approach in analysis of bivariate data*, in B. Schelter, M. Winterhalder, and J. Timmer (Eds.), Handbook of Time Series Analysis, Wiley-VCH, pp. 159 – 180, 2006
[35] O.E. Rössler, *An equation for continuous chaos*, Physics Letters, Vol. 57A, No. 5, pp. 397 – 398, 1976
[36] M.A.F. Sanjuán, *The effect of nonlinear damping on the universal escape oscillator*, International Journal of Bifurcation and Chaos, Vol. 9, No. 4, pp. 735 – 744, 1999
[37] W.E. Sherwood and J. Guckenheimer, *Dissecting the phase response of a model bursting neuron*, SIAM Journal on Applied Dynamical Systems, Vol. 9, No. 3, pp. 659 – 703, 2010
[38] M. Spivak, *A Comprehensive Introduction to Differential Geometry*, 2$^{\text{nd}}$ Edition, Berkeley, CA: Publish or Perish Press, 1979
[39] D.C. Soriano, E.Z. Nadalin, R. Suyama, J.M.T. Romano and R. Attux, *Chaotic convergence of the decision-directed blind equalization algorithm*, Communications in Nonlinear Science and Numerical Simulation, Vol. 17, No. 12, pp. 5097 – 5109, December 2012
[40] L.A.B. Tôrres and L.A. Aguirre, *Transmitting information by controlling nonlinear oscillators*, Physica D, Vol. 196, pp. 387 – 406, 2004
[41] T. Uehara, T. Tanaka and S. Fiori, *Robust averaging of covariance matrices for motor-imagery brain-computer interfacing by Riemannian geometry*, in Proc. of the 5$^{\text{th}}$ International Conference on Cognitive Neurodynamics (ICCN 2015, Sanya, China, June 3-7, 2015), pp. 347 – 353, January 2016
[42] J.D. Velásquez Henao, *An introduction to chaos-based algorithms for numerical optimization*, Revista Avances en Sistemas e Informática (ISSN: 1657-7663), Vol. 8, No. 1, pp. 51 – 60, March 2011
[43] B. Wang, S.M. Zhong and X.C. Dong, *On the novel chaotic secure communication scheme design*, Communications in Nonlinear Science and Numerical Simulation, Vol. 39, pp. 108 – 117, October 2016
[44] L. Wang, Z. Meng, Y. Sun, L. Guo and M. Zhou, *Design and analysis of a novel chaotic diagonal recurrent neural network*, Communications in Nonlinear Science and Numerical Simulation, Vol. 26, No.s 1–3, pp. 11 – 23, September 2015
[45] X. Wua, B. Wanga, W. Shi and X. You, *On extended RKN integrators for multidimensional perturbed oscillators with applications*, Applied Mathematical Modelling, Vol. 36, pp. 1504 – 1513, 2012
[46] D. Yang, Z. Liu and J. Zhou, *Chaos optimization algorithms based on chaotic maps with different probability distribution and search speed for global optimization*, Communications in Nonlinear Science and Numerical Simulation, Vol. 19, No. 4, pp. 1229 – 1246, April 2014
[47] J.-P. Yeh and K.-L. Wu, *A simple method to synchronize chaotic systems and its application to secure communications*, Mathematical and Computer Modelling, Vol. 47, pp. 894 – 902, 2008
[48] J. Yoo and S. Choi, *Orthogonal nonnegative matrix factorization: multiplicative updates on Stiefel manifolds*, Proc. of the Intelligent Data Engineering and Automated Learning (IDEAL 2008), Springer Berlin/Heidelberg, pp. 140 – 147, 2008
[49] X. Wu, B. Wang, W. Shi and X. You, *On extended RKN integrators for multidimensional perturbed oscillators with applications*, Applied Mathematical Modelling, Vol. 36, pp. 1504 – 1513, 2012
[50] R. Zimmermann, *A matrix-algebraic algorithm for the Riemannian logarithm on the Stiefel manifold*. Public report available from the arXiv website (`https://arxiv.org/abs/1604.05054`), dated April 2016

Appendix A. Detailed derivation of the Lorenz-like model on the unit sphere. Upon introducing the state-vector $z = [z_1 \ z_2 \ z_3]^T \in \mathbb{R}^3$, the Lorenz oscillator may be expressed by the following system of three non-linear differential equations:

$$\left\{ \begin{array}{rcl} \dot{z}_1 & = & \sigma(z_2 - z_1), \\ \dot{z}_2 & = & \rho z_1 - z_1 z_3 - z_2, \\ \dot{z}_3 & = & z_1 z_2 - \beta z_3, \end{array} \right. \tag{A.1}$$

equipped with the initial conditions $z_1(0) = z_{10}$, $z_2(0) = z_{20}$ and $z_3(0) = z_{30}$. The constant σ denotes the Prandtl number and the constant ρ denotes the Rayleigh number. The first-order system (A.1) can be represented as a second-order dynamical system by taking the time-derivative of both sides of the

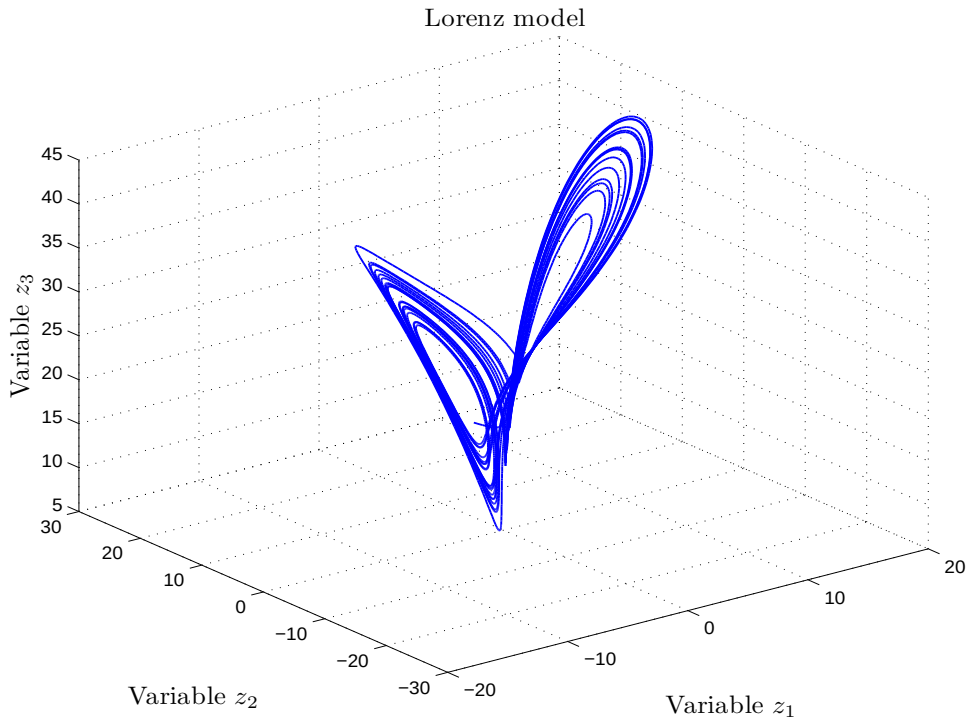

FIG. A.1. *Exemplary behavior of a Lorenz model in terms of the three variables* $(z_1, z_2, z_3) \in \mathbb{R}^3$.

equations (A.1), that leads to:

$$\left\{ \begin{array}{rcl} \dot{z} & = & w,\ w = [w_1\ w_2\ w_3]^T \in \mathbb{R}^3, \\ \dot{w} & = & -C(z)w,\ C(z) \stackrel{\text{def}}{=} \left[\begin{array}{ccc} \sigma & -\sigma & 0 \\ z_3 - \rho & 1 & z_1 \\ -z_2 & -z_1 & \beta \end{array} \right], \end{array} \right. \tag{A.2}$$

equipped with the initial conditions $z_1(0) = z_{10}$, $z_2(0) = z_{20}$ and $z_3(0) = z_{30}$, $w_1(0) = \sigma(z_{20} - z_{10})$, $w_2(0) = \rho z_{10} - z_{10} z_{30} - z_{20}$ and $w_3(0) = z_{10} z_{20} - \beta z_{30}$. The Figure A.1 illustrates the state of a Lorenz model in terms of the three variables $(z_1, z_2, z_3) \in \mathbb{R}^3$.

The Lorenz system (A.1) or (A.2) generates a trajectory $z(t)$ evolving freely in the space $\mathbb{R}^3$ and forming a complex, non-repeating, three-dimensional curve. In order to reformulate the Lorenz system on a three-dimensional sphere S^2, it pays to define a new variable as

$$x \stackrel{\text{def}}{=} \frac{z}{\|z\|}, \tag{A.3}$$

where the symbol $\|\cdot\|$ denotes again the standard vector 2-norm, namely $\|z\| \stackrel{\text{def}}{=} \sqrt{z^T z}$. In order to formulate the sought Lorenz system on the manifold S^2, we start from seeking the law governing the evolution of the acceleration $\ddot{x}$. Note that, at any time, it holds that $x^T x = 1$.

Let us start by computing the first-order derivative of the variable $x(t)$ with respect to the parameter t. It is understood that the manifold S^2 is embedded into the ambient space $\mathbb{R}^3$. Note that

$$\frac{\mathrm{d}}{\mathrm{d}t}\|z\| = \frac{\mathrm{d}}{\mathrm{d}t}(z^T z)^{\frac{1}{2}} = \tfrac{1}{2}(z^T z)^{-\frac{1}{2}} 2 \dot{z}^T z = \frac{\dot{z}^T z}{\|z\|}. \tag{A.4}$$

Consequently, we have that:

$$\dot{x} = \frac{\dot{z}\|z\| - z(\mathrm{d}\|z\|/\mathrm{d}t)}{\|z\|^2} = \frac{\dot{z}}{\|z\|} - \frac{z(\dot{z}^T z)}{\|z\|^3} = (I - xx^T)\frac{\dot{z}}{\|z\|}, \tag{A.5}$$

where I denotes a 3×3 identity matrix. Note that $x^T \dot{x} = 0$. By deriving both sides of the equation (A.5) with respect to the parameter t, we get:

$$\ddot{x} = (-\dot{x}x^T - x\dot{x}^T)\frac{\dot{z}}{\|z\|} + (I - xx^T)\frac{\mathrm{d}}{\mathrm{d}t}\left(\frac{\dot{z}}{\|z\|}\right). \tag{A.6}$$

Note that:

$$\frac{\mathrm{d}}{\mathrm{d}t}\left(\frac{\dot{z}}{\|z\|}\right) = \frac{\ddot{z}\|z\| - \dot{z}(\dot{z}^T z/\|z\|)}{\|z\|^2} = \frac{\ddot{z}}{\|z\|} - \frac{\dot{z}\dot{z}^T x}{\|z\|^2},$$

where the equation (A.4) has been used again. Consequently, it holds that:

$$(I - xx^T)\frac{\mathrm{d}}{\mathrm{d}t}\left(\frac{\dot{z}}{\|z\|}\right) = \frac{\ddot{z}}{\|z\|} - \frac{\dot{z}x^T\dot{z}}{\|z\|^2} - \frac{xx^T\ddot{z}}{\|z\|} + \frac{x(x^T\dot{z})^2}{\|z\|^2}.$$

Plugging the last expression into the derivative (A.6) yields:

$$\ddot{x} = -\frac{\dot{x}x^T\dot{z}}{\|z\|} - \frac{x\dot{x}^T\dot{z}}{\|z\|} + \frac{\ddot{z}}{\|z\|} - \frac{\dot{z}x^T\dot{z}}{\|z\|^2} - \frac{xx^T\ddot{z}}{\|z\|} + \frac{x(x^T\dot{z})^2}{\|z\|^2}. \tag{A.7}$$

Note that the matrix $I - xx^T$ is an orthogonal projector from $\mathbb{R}^3$ to $T_x\mathrm{S}^2$, therefore, the equation (A.5) tells that the vector $\dot{x}$ is an orthogonal projection of the vector $\frac{\dot{z}}{\|z\|}$ over $T_x\mathrm{S}^2$. Consequently, one may write the quantity $\dot{z}$ as a linear combination of the tangent component $\dot{x}$ and of the normal component x as

$$\dot{z} = \|z\|\dot{x} + \bar{\lambda}x, \text{ with } \bar{\lambda} \in \mathbb{R} \text{ arbitrary.}$$

It follows that some terms in the right-hand side of the expression (A.7) may be simplified as shown below:

$$\begin{aligned}
\frac{\dot{x}x^T\dot{z}}{\|z\|} &= \frac{\dot{x}x^T\dot{x}\|z\| + \bar{\lambda}\dot{x}}{\|z\|} = \frac{\bar{\lambda}\dot{x}}{\|z\|}, \\
\frac{x\dot{x}^T\dot{z}}{\|z\|} &= \frac{x\dot{x}^T\dot{x}\|z\| + \bar{\lambda}x\dot{x}^T x}{\|z\|} = x\|\dot{x}\|^2, \\
\frac{\dot{z}x^T\dot{z}}{\|z\|^2} &= \frac{(\dot{x}\|z\| + \bar{\lambda}x)\bar{\lambda}}{\|z\|^2} = \frac{\bar{\lambda}\dot{x}}{\|z\|} + \frac{\bar{\lambda}^2 x}{\|z\|^2}, \\
\frac{x(x^T\dot{z})^2}{\|z\|^2} &= \frac{\bar{\lambda}^2 x}{\|z\|^2},
\end{aligned}$$

where the properties $x^T x = 1$ and $x^T\dot{x}$ have been used repeatedly. From the system (A.2), we may also write:

$$\ddot{z} = -C(z)\dot{z} = -C(z)(\dot{x}\|z\| + \bar{\lambda}x).$$

Plugging the last expressions into the formula (A.7) gives:

$$\ddot{x} = -(I - xx^T)\frac{C(z)\dot{z}}{\|z\|} - x\|\dot{x}\|^2 - \frac{2\bar{\lambda}\dot{x}}{\|z\|}. \tag{A.8}$$

Let us analyze, in details, the three terms on the right-hand side of the equation (A.8):

- The term $-x\|\dot{x}\|^2$ is precisely the Christoffel term predicted in the equation (3.7).
- The quantity $\|z\|$ is exogenous with respect to the chaotic oscillator and is replaced by a constant $\nu > 0$ in the present example. Then, in the term $\frac{2\bar{\lambda}\dot{x}}{\|z\|}$, it is assumed as absorbed by the constant $\lambda \stackrel{\text{def}}{=} \frac{\bar{\lambda}}{\nu}$, which is arbitrary. The resulting term $-2\lambda\dot{x}$ represents an instance of the friction-type damping discussed in the Subsection 2.2.
- The addendum $-(I - xx^T)\frac{C(z)\dot{z}}{\|z\|}$ is the Lorenz term and may be further elaborated as follows. Note that $C(z) = A + B(z)$, where the constant 3×3 matrix A and the matrix-function $B(z)$ are defined as in (4.2), namely:

$$A \stackrel{\text{def}}{=} \begin{bmatrix} \sigma & -\sigma & 0 \\ -\rho & 1 & 0 \\ 0 & 0 & \beta \end{bmatrix}, \; B(z) \stackrel{\text{def}}{=} \begin{bmatrix} 0 & 0 & 0 \\ z_3 & 0 & z_1 \\ -z_2 & -z_1 & 0 \end{bmatrix}.$$

  The matrix-function $B(z)$ is linear in z, hence, setting $z = \nu x$ from (A.3), one may write $C(z) = A + \nu B(x)$, therefore:

$$-(I - xx^T)\frac{C(z)\dot{z}}{\|z\|} = (xx^T - I)[A + \nu B(x)]\frac{\nu\dot{x} + \bar{\lambda}x}{\nu} = (xx^T - I)[A + \nu B(x)]\left(\dot{x} + \lambda x\right),$$

  that is the final expression of the Lorenz term.

In conclusion, the Lorenz oscillator on the unit sphere takes on the form expressed in the equations (4.3) and (4.4).